Available online at www.sciencedirect.com
ScienceDirect
Biochemical and Biophysical Research Communications 358 (2007) 203–208
BBRC
www.elsevier.com/locate/ybbrc

Simple quantitative detection of mitochondrial superoxide production in live cells

Partha Mukhopadhyay [a], Mohanraj Rajesh [a], Kashiwaya Yoshihiro [b], György Haskó [c], Pál Pacher [a,*]

[a] Section on Oxidative Stress Tissue Injury, Laboratory of Physiological Studies, National Institutes of Health/NIAAA, Bethesda, MD 20892-9413, USA
[b] Laboratory of Metabolic Control, National Institutes of Health/NIAAA, Bethesda, MD 20892-9413, USA
[c] Department of Surgery, UMDNJ-New Jersey Medical School, Newark, NJ 07103, USA

Received 12 April 2007
Available online 25 April 2007

Abstract

Experiments with isolated mitochondria have established that these organelles are pivotal intracellular sources of superoxide in a variety of pathophysiological conditions. Recently, a novel fluoroprobe MitoSOX Red was introduced for selective detection of superoxide in the mitochondria of live cells and was validated with confocal microscopy. Here we show ~3–7 fold dose- and time-dependent increase in mitochondrial superoxide production (measured by MitoSOX using flow cytometry and confocal microscopy) in rat cardiac derived H9c2 myocytes and/or in human coronary artery endothelial cells triggered by Antimycin A, Paraquat, Doxorubicin or high glucose. These results establish a novel, quantitative method for simple detection of mitochondrial superoxide generation simultaneously in a large population of live cells by flow cytometry. This method can also be adapted for immune cell studies with mixed population of T or B cells or their subsets to analyze mitochondrial superoxide levels using multiple labeled surface markers in individual populations. Published by Elsevier Inc.

Keywords: Superoxide; Mitochondria; Free radicals; MitoSOX; Antimycin A (AntA); Paraquat (PQ); Doxorubicin (DOX); Cardiomyocytes; H9c2; Human coronary artery endothelial cells (HCAECs)

The recognition that the free radical superoxide anion could be a biologically significant molecule has stimulated an extraordinary impetus for scientific research in all the fields of biology and medicine [1–3]. Under various pathological conditions several enzyme complexes, such as xanthine and NAD(P)H oxidases can be activated in many cellular systems to produce large amounts of superoxide [4,5]. There is increasing evidence (based mostly on experiments derived from isolated mitochondria) suggesting that mitochondrial dysfunction and interrelated intramitochondrial generation of superoxide anion and other reactive oxygen and nitrogen species (ROS and RNS) are also implicated in the pathophysiological processes associated with aging, cancer, neurodegenerative and inflammatory disorders, diabetes, and diabetic complications [6–9]. The recognition of the pivotal role of the mitochondria in the generation of ROS rekindled significant interest in the development of methods to assess the mitochondrial superoxide generation, which was largely hampered by the lack of a sensitive and specific assay [10–12]. Recently, a novel fluoroprobe MitoSOX Red (MitoSOX) was introduced for selective detection of superoxide in the mitochondria of live cells, and was validated with fluorescent microscopy [11]. However, this method allows only semiquantitative detection of the mitochondrial superoxide generation in a relatively few cells simultaneously. Therefore, we aimed to develop a simple and quantitative method for detection of the mitochondrial superoxide generation simultaneously in a large population of live cells with MitoSOX using flow cytometry. Although we used cardiac derived rat H9c2

* Corresponding author. Fax: +1 301 480 0257.
E-mail address: pacher@mail.nih.gov (P. Pacher).

0006-291X/$ - see front matter Published by Elsevier Inc.
doi:10.1016/j.bbrc.2007.04.106

myocytes and human coronary artery endothelial cells (HCAECs) as a model systems to study the mitochondrial superoxide production in live cells, this method can easily be adapted for virtually any cell types.

Materials and methods

Reagents and cell culture. Antimycin A (AntA), Paraquat (PQ), Doxorubicin hydrochloride (DOX), D-glucose, D-mannitol, and BSA (cell culture grade) were purchased from Sigma Chemical (St. Louis, MO). MitoSOX [3,8-phenanthridinediamine, 5-(6′-triphenylphosphonium-hexyl)-5,6 dihydro-6-phenyl] was purchased from Molecular Probes (Invitrogen, Carlsbad, CA).

Rat embryonic ventricular myocardial H9c2 cells were obtained from American Type Culture Collection (Manassas, VA). Cells were cultured in 12 well cell culture plates or glass bottom dishes (MatTek , Ashland, MA) with DMEM (Gibco, Invitrogen, Carlsbad, CA) containing 10% fetal bovine serum (Invitrogen, Carlsbad, CA), 100 U/ml penicillin and 100 μg/ml streptomycin at 37 °C in a humidified atmosphere of 5% CO_2 as previously described [13,14]. Cells were always used at less than 80% of confluence.

Human coronary artery endothelial cells (HCAEC) were purchased from Cell Applications, Inc. (San Diego, CA). HCAEC were grown in HCAEC growth medium in 12 well cell culture plates or glass bottom dishes coated with 0.2% gelatin. HCAEC were used between passages 4 and 6 for the experiments. The cells were maintained at 37 °C in humidified 5% CO_2 incubator.

Acute treatment with Antimycin A, Paraquat, and Doxorubicin of H9c2 cardimyocytes. Cell were grown till 50–80% confluence and the fresh media were added before experiments. MitoSOX was added to final concentration of 5 μM according to manufacturer's recommendation. Cells were allowed to load MitoSOX for 30 min and the cells were washed two times with Hank's Buffered Salt Solution (HBSS) containing calcium and magnesium. For confocal microscopy, cells in glass bottom dishes were treated with 100 μM AntimycinA or 100 μM Paraquat or 20 μM Doxorubicin in HBSS (with Ca/Mg) containing 1% BSA. PBS was used in control treatment for each set. Cells were kept 30 min in CO_2 incubator at 37 °C before analysis in confocal microscope as described below. For flow cytometry analysis, after 30 min loading of MitoSOX, H9c2 cells in cell culture dishes were trypsinized for 2 min and neutralized with media. Cells were washed with HBSS (with Ca/Mg) containing 1% BSA and suspended at a density of $1–2 \times 10^7$/cells/ml. Cells were aliquoted at $5–10 \times 10^6$ cells in sterile FACS tube and treated with 50 or 100 μM Antimycin A or 50 or 100 μM Paraquat and 10, 20 or 50 μM Doxorubicin in HBSS (with Ca/Mg) containing 1% BSA. Flow cytometry was performed at different time points as described where appropriate. Cells were kept in CO_2 incubator at 37 °C between measurements. Triplicates experiments were carried out for each set.

Chronic treatment with Doxorubicin of H9c2 cardimyocytes. In a separate set of experiments, H9c2 cells were treated with PBS or Doxorubicin at 1 μM for 24 h in CO_2 incubator at 37 °C in 12 well plate or glass bottom dishes. For confocal microscopy, MitoSOX was added at 5 μM in the medium after treatment for 20 min and cells were washed before measurement. Cells were trypsinized for 2 min after 20 min MitoSOX loading for flow cytometry measurement.

Treatment with high glucose of human coronary endothelial cells. HCAECs were seeded in 0.2% gelatin coated 12 well culture plates or glass bottom dishes and allowed to reach confluence. Then cells were pre-conditioned in growth factor free medium containing 2% FBS for 4 h, followed by treatments for 48 h either with PBS, 5 mM D-glucose, 30 mM D-glucose or 30 mM D-mannitol (osmotic control) for 48 h. At the end of incubation, MitoSOX 5.0 μM was added to the cells and incubated further for 20 min at 37 °C in 5% CO_2 atmosphere. Subsequently, cells were collected by trypsinization, washed in HBSS (with Ca/Mg) supplemented with 1% BSA and measurements were performed for flow cytometry. Cells in glass bottom dishes were washed as stated before after 20 min MitoSOX loading and used for confocal microscopy imaging.

Confocal microscopy with MitoSOX. The digital images were taken by an inverted confocal laser scanning microscope LSM Pascal (Zeiss, Germany) at 2048×2048 pixels. Images were captured using either 40× or 100× oil immersion objective lens and optical section was <1 μm. MitoSOX was excited by laser at 514 nm as described [11].

Flow cytometry with MitoSOX. For the determination of mitochondrial superoxide by flow cytometry, the measurements were carried out using FAScalibur (BD Bioscience, San Jose, CA). MitoSOX Red was excited by laser at 488 nm, a similar excitation (514 nm) used in confocal studies [11] and the data collected at FSC, SSC, 585/42 nm (FL2) and 670LP(FL3) channel. In this study, the data were presented in the FL2 channel. Cell debris as represented by distinct low forward and side scatter were gated out for analysis. The data presented by histogram of mean intensity of MitoSOX fluorescence or fold change when compared with PBS control with MitoSOX present.

Statistical analysis All the values are represented as means ± standard deviation. Statistical significance of the data was assessed by paired Student's *t*-test or one-way ANOVA as appropriate. $P < 0.05$ was considered significant.

Results

Antimycin A (AntA) dose- and time-dependently increased mitochondrial superoxide generation in cardiomyocytes

Confocal microscopic imaging demonstrated significant increase in mitochondrial fluorescence intensity of MitoSOX in H9c2 cells treated with 100 μM Antimycin A (Fig. 1A). Histograms of FACS analysis showed marked increase of mean intensity with increasing concentrations of Antimycin A (Fig. 1B). As a negative control PBS or 50 μM Antimycin A without MitoSOX were used. Quantitative measurements of the mean fluorescence intensities from the samples demonstrated 4.6 ± 0.12 and 5.5 ± 0.17 fold increase in MitoSOX fluorescence intensity with 50 μM and 100 μM Antimycin A following 1 h treatment (Fig. 1C). MitoSOX fluorescence was increased with Antimycin A both in a dose- and time-dependent manner (Fig. 1D).

Paraquat (PQ) dose- and time-dependently increased mitochondrial superoxide generation in H9c2 cardimyocytes

Confocal microscopic imaging demonstrated significant increase in mitochondrial fluorescence intensity of MitoSOX in H9c2 cells treated with 100 μM Paraquat (Fig. 2A). Histograms of FACS analysis showed increase of mean intensity with increasing concentrations of Paraquat (Fig. 2B). As a negative control PBS or 50 μM Paraquat without MitoSOX were used. Quantitative measurements of the mean fluorescence intensities from the samples demonstrated 3.7 ± 0.13 and 6.9 ± 0.32 fold increased with 50 μM and 100 μM Paraquat following 1 h treatment, respectively (Fig. 2C). MitoSOX fluorescence was increased with Paraquat both in a dose- and time-dependent manner (Fig. 2D).

Doxorubicin (DOX) dose- and time-dependently increased mitochondrial superoxide generation in H9c2 cardimyocytes

Confocal microscopic imaging demonstrated significant increase in mitochondrial fluorescence intensity of

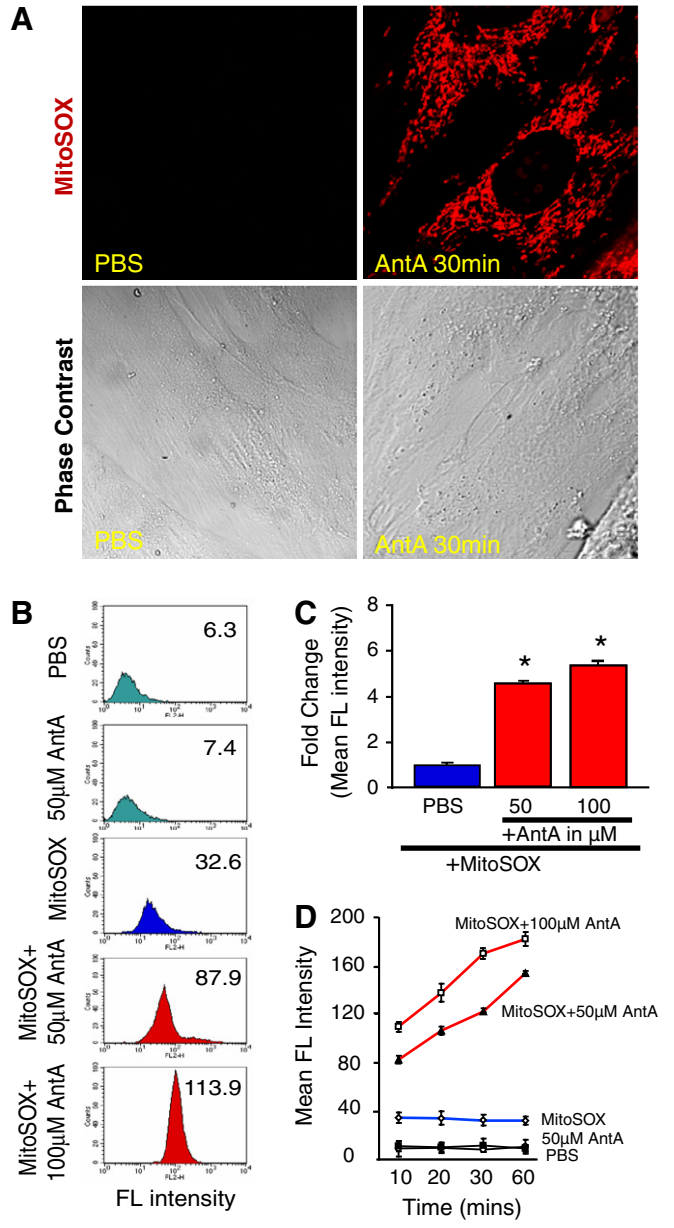

Fig. 1. Antimycin A increases mitochondrial superoxide formation in H9c2 myocytes. (A) Representative confocal images of H9c2 cells showing increase in mitochondrial MitoSOX fluorescence following treatment with antimycin A at 100 μM for 30 min. (B) Representative histograms of flow cytometry experiments demonstrating dose-dependent increase in mean fluorescent intensity of oxidized MitoSOX following antimycinA pre-treatment as indicated. (C,D) Quantitative data expressing dose- and time-dependent changes in mean fluorescent intensity of MitoSOX following antimycin A exposure measured by flow cytometry. Data presented as average ± standard deviation, $n = 3$. $^{*}P < 0.01$ vs PBS + MitoSOX, $n = 3$.

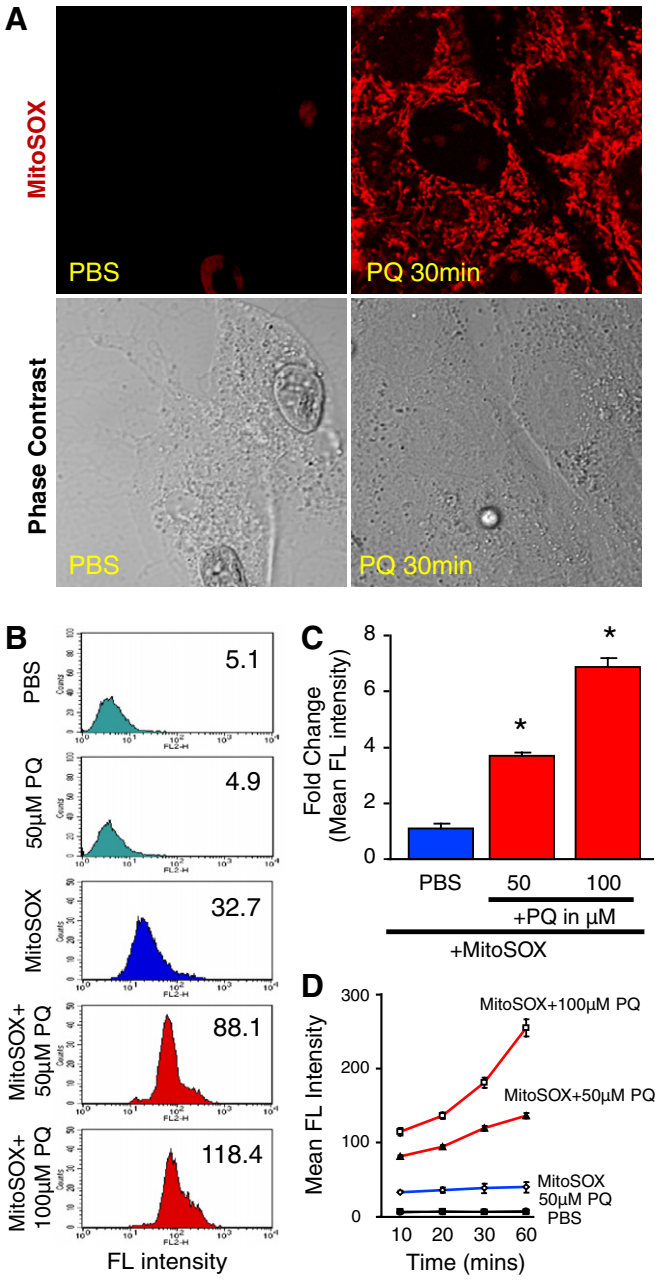

Fig. 2. Paraquat (PQ) increases mitochondrial superoxide formation in H9c2 myocytes. (A) Representative confocal images of H9c2 cells showing increase in mitochondrial MitoSOX fluorescence following treatment with PQ at 100 μM for 30 min. (B) Representative histograms of flow cytometry experiments demonstrating dose-dependent increase in mean fluorescent intensity of MitoSOX following PQ pretreatment as indicated. (C,D) Quantitative data expressing dose- and time-dependent changes in mean fluorescent intensity of MitoSOX following PQ exposure measured by flow cytometry. Data presented as average ± standard deviation, $n = 3$. $^{*}P < 0.01$ vs PBS + MitoSOX, $n = 3$.

MitoSOX in H9c2 cells treated with 20 μM DOX for 0.5 h (Fig. 3A). Histograms of FACS analysis showed dose-dependent increase of mean fluorescence intensity of MitoSOX with increasing concentrations of DOX (Fig. 3B). As a negative control PBS or 10 μM DOX were used. Notable, DOX alone (unlike Ant A or PQ, see Figs. 1 and 2) induced a small increase in fluorescence (most likely because of the autofluorescence). Quantitative measurements of the mean intensities from the samples demonstrated 1.4 ± 0.04, 1.8 ± 0.08, and 2.8 ± 0.08 fold increased with 10 μM, 20 μM, and 50 μM DOX, respectively, following 1 h treatment (Fig. 3C). MitoSOX fluorescence was increased with DOX both in a dose- and time-dependent fashion (Fig. 3D).

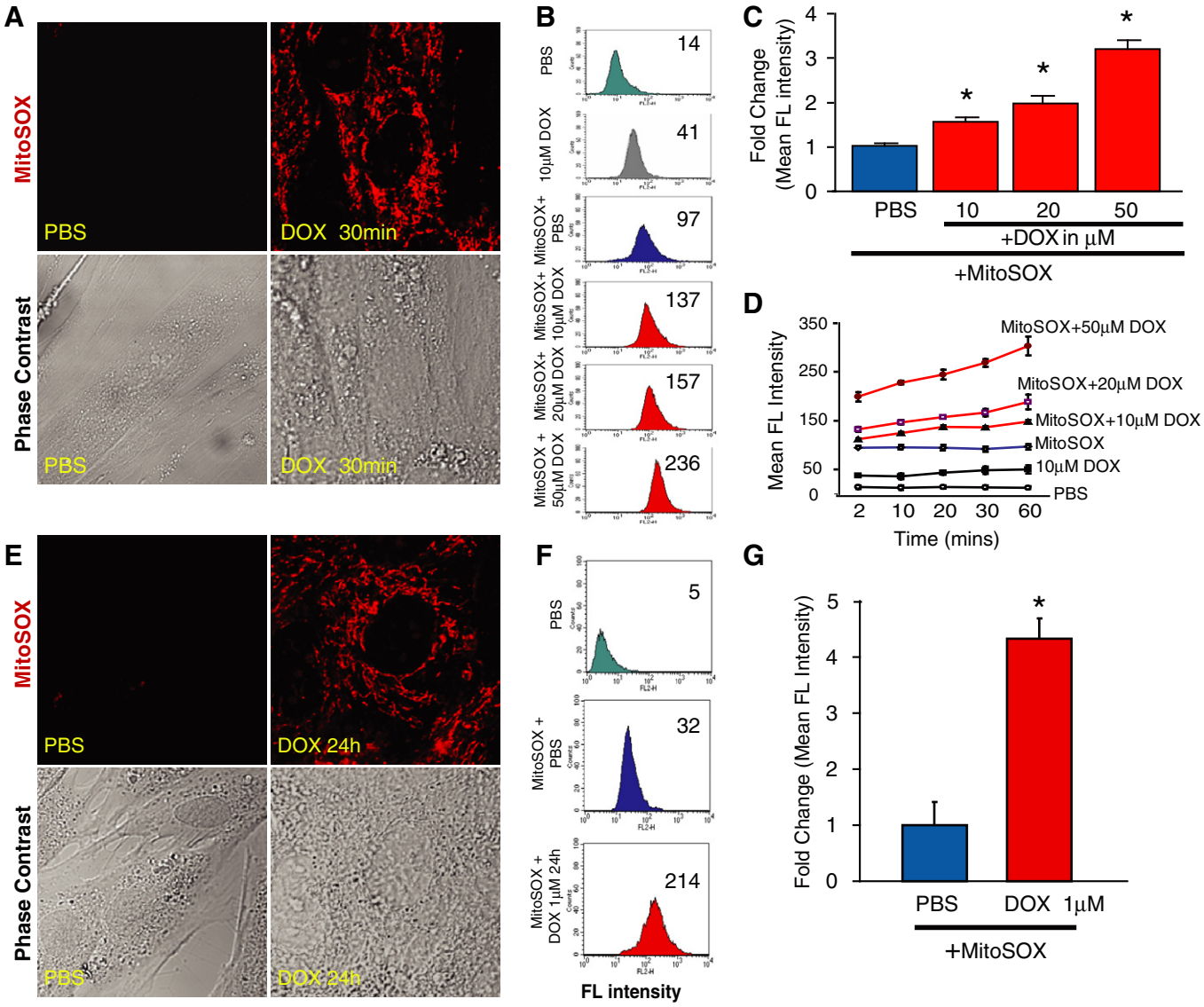

Fig. 3. Doxorubicin (DOX) increases mitochondrial superoxide formation in H9c2 myocytes. (A,E) Representative confocal images of H9c2 cells showing increase in mitochondrial MitoSOX fluorescence following acute or chronic treatment with DOX at 20 μM for 30 min (A) or 1 μM for 24 h (E). (B,F) Representative histograms of flow cytometry experiments demonstrating increase in mean fluorescent intensity of MitoSOX following DOX pretreatments as indicated. (C, D, and G) Quantitative data expressing dose- and time-dependent changes in mean fluorescent intensity of MitoSOX following DOX exposure measured by flow cytometry as indicated. Data presented as average ± standard deviation, $n = 3$. $^{*}P < 0.01$ vs PBS + MitoSOX, $n = 3$.

Confocal microscopic imaging demonstrated significant increase in mitochondrial fluorescence of MitoSOX in H9c2 cells treated with 1 μM DOX for 24 h (Fig. 3E). Histograms of FACS analysis showed significant increase of mean fluorescence intensity of MitoSOX following DOX treatment (Fig. 3F). Quantitative measurements of the mean intensity from the samples demonstrated 4.3 ± 0.37 fold increased with 1 μM DOX after 24 h treatment (Fig. 3G).

High glucose exposure increased mitochondrial superoxide generation in human coronary artery endothelial cells

Confocal microscopic imaging demonstrated markedly increased mitochondrial fluorescence intensity of MitoSOX in HCAECs treated with 30 mM D-glucose (but not 30 mM D-mannitol (osmotic control)) for 48 h, compared to normal glucose (5 mM) or PBS (Fig. 4A).

Histograms of FACS analysis showed significant increase of mean fluorescence intensity of MitoSOX following 30 mM D-glucose treatment (Fig. 3B). Quantitative measurements of the mean intensity from the samples demonstrated markedly enhanced mitochondrial superoxide generation in HCAEC (Fig. 4B, C). Quantitative measurements of the mean intensity from the samples demonstrated 3.8 ± 0.39 fold increased with 30 mM D-glucose following 48 h treatment (Fig. 4C).

Discussion

MitoSOX Red is a novel fluorogenic dye recently developed and validated [11] for highly selective detection of

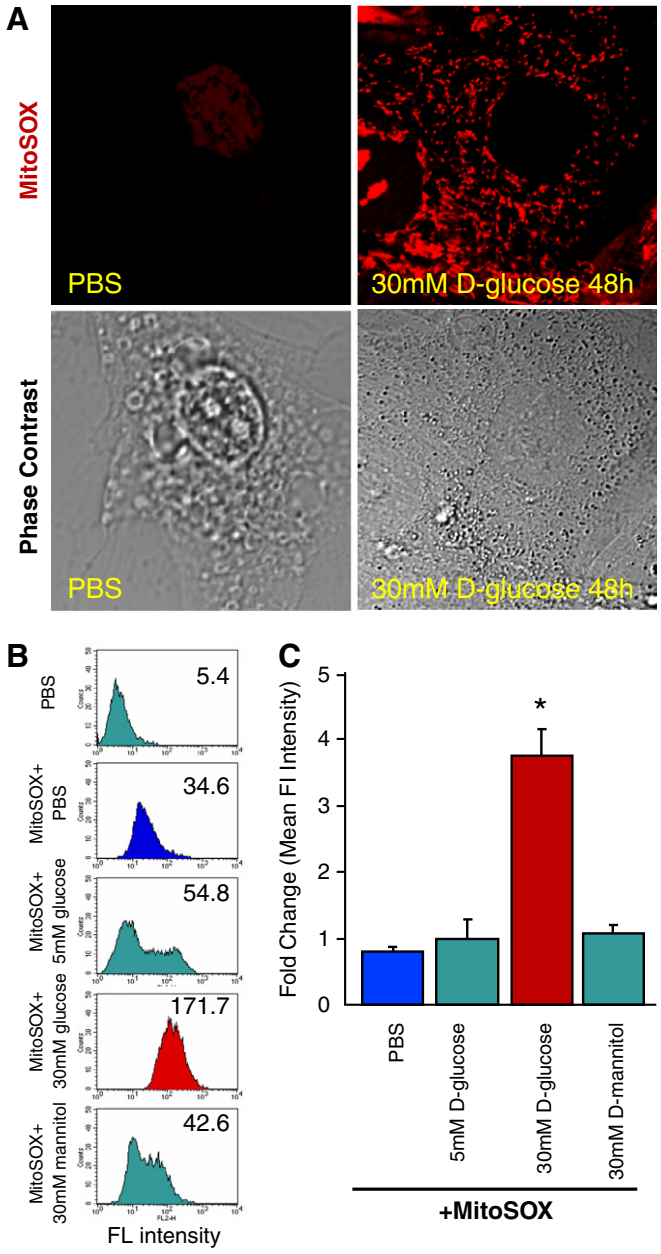

Fig. 4. High glucose increases mitochondrial superoxide formation in HCAECs. (A) Representative confocal images of HCAEC cells showing increase in mitochondrial MitoSOX fluorescence following treatment with 30 mM glucose for 48 h. (B) Representative histograms of flow cytometry experiments demonstrating increase in mean fluorescent intensity of MitoSOX following high glucose pretreatment as indicated. (C) Quantitative data showing fold increase of mean intensity with high glucose as described. Data presented as average ± standard deviation, $n = 3$. $^{*}P < 0.01$ vs 5 mM glucose + MitoSOX, $n = 3$.

superoxide in the mitochondria of live cells. Numerous recent studies utilizing different stimuli of superoxide production coupled with fluorescent microscopy have demonstrated detectable changes with MitoSOX in mitochondrial superoxide generation in olygodendrocytes [11], retinal ganglion cells [15], neurons [16,17], isolated cardiomyocytes [18], and parasite *Trypanosoma cruzi* [19].

However, the disadvantage of the fluorescent microscopy technique is that it allows measurements of various biological processes only in a relatively limited number of cells simultaneously, and is semiquantitative. In addition, cells loaded with fluorescent probes during the fluorescent microscopy receive more exposure of lasers or UV, which can increase ROS generation by itself, than during the flow cytometry experiments.

In the present study, we demonstrate using well-established stimuli of mitochondrial superoxide and ROS production such as mitochondrial complex III inhibitor Antimycin A [11], herbicide paraquat [11,20], chemotherapeutic agent Doxorubicin (known for its cardiotoxicity; [21,22]) and high glucose [23], a marked ~3–7 fold dose- and time-dependent augmentation of mitochondrial superoxide generation measured by increased fluorescent intensity of MitoSOX by flow cytometry. In these experiments the mitochondrial superoxide generation measured by MitoSOX could largely be prevented by pretreatment of cells with high concentrations of cell permeable SOD (data not shown) as previously described [11]. These results are also in well-agreement with previous reports demonstrating increased superoxide and/or other ROS generation either in isolated mitochondria exposed to these pathologically relevant stimuli or in cells loaded with cytosolic ROS detecting probes ([20–23]; in most of the later experiments the mitochondrial contribution to ROS/superoxide production was deduced from the use of various mitochondrial uncouplers (known also to dissipate mitochondrial membrane potential)), and with a recent fluorescent microscopy study using MitoSOX [11] along with the confocal microscopy data shown in the present manuscript.

One possible limitation of the detection of mitochondrial superoxide production using MitoSOX is that it can bind to the nuclear DNA following oxidation. This could be minimized with individual optimization of loading conditions for each cell type and normalization of the data to the control cells loaded with MitoSOX. Another possible limitation is that under various conditions, where increased cytosolic superoxide generation may also be enhanced in addition to the mitochondrial (and is already present at a time of the loading with MitoSOX) some of the MitoSOX may be oxidized during the transport from cell membrane before entering into the mitochondria. In theory, superoxide produced from the mitochondria can also diffuse to and present in the cytosol contributing to similar scenario during the loading. However, as clearly demonstrated by our chronic treatment protocols with high glucose and Doxorubicin in endothelial cells and/or myocytes (supported by confocal microscopy data), this level of cytosolic oxidized MitoSOX is likely to be negligible in comparison with the increase in fluorescence detected in the mitochondria.

Collectively, these results establish a new method allowing simple, selective and quantitative detection of the mitochondrial superoxide generation simultaneously in a large number of live cells by flow cytometry, which can easily

be applicable for virtually any cell types. The clear advantages of this method over other cell-based techniques and fluorescent microscopy are: tremendous speed, exquisite precision, and possibility of simultaneous quantitative measurements of multiple cellular parameters with maximal preservation of cell viability and cellular functions.

Acknowledgments

This study was supported by the Intramural Research Program of NIH/NIAAA (to P.P.). Authors are indebted to Professor Joseph S. Beckman for reading the manuscript and valuable comments.

References

[1] I. Fridovich, Superoxide radical: an endogenous toxicant, Annu. Rev. Pharmacol. Toxicol. 23 (1983) 239–257.
[2] I. Fridovich, Biological effects of the superoxide radical, Arch. Biochem. Biophys. 247 (1986) 1–11.
[3] I. Fridovich, Superoxide radical and superoxide dismutases, Annu. Rev. Biochem. 64 (1995) 97–112.
[4] K.K. Griendling, D. Sorescu, M. Ushio-Fukai, NAD(P)H oxidase: role in cardiovascular biology and disease, Circ. Res. 86 (2000) 494–501.
[5] P. Pacher, A. Nivorozhkin, C. Szabo, Therapeutic effects of xanthine oxidase inhibitors: renaissance half a century after the discovery of allopurinol, Pharmacol. Rev. 58 (2006) 87–114.
[6] M.K. Shigenaga, T.M. Hagen, B.N. Ames, Oxidative damage and mitochondrial decay in aging, Proc. Natl. Acad. Sci. USA 91 (1994) 10771–10778.
[7] K. Green, M.D. Brand, M.P. Murphy, Prevention of mitochondrial oxidative damage as a therapeutic strategy in diabetes, Diabetes 53 (Suppl 1) (2004) S110–S118.
[8] A. Csiszar, P. Pacher, G. Kaley, Z. Ungvari, Role of oxidative and nitrosative stress, longevity genes and poly(ADP-ribose) polymerase in cardiovascular dysfunction associated with aging, Curr. Vasc. Pharmacol. 3 (2005) 285–291.
[9] P. Pacher, J.S. Beckman, L. Liaudet, Nitric oxide and peroxynitrite in health and disease, Physiol. Rev. 87 (2007) 315–424.
[10] A. Gomes, E. Fernandes, J.L. Lima, Fluorescence probes used for detection of reactive oxygen species, J. Biochem. Biophys. Methods 65 (2005) 45–80.
[11] K.M. Robinson, M.S. Janes, M. Pehar, J.S. Monette, M.F. Ross, T.M. Hagen, M.P. Murphy, J.S. Beckman, Selective fluorescent imaging of superoxide in vivo using ethidium-based probes, Proc. Natl. Acad. Sci. USA 103 (2006) 15038–15043.
[12] N. Soh, Recent advances in fluorescent probes for the detection of reactive oxygen species, Anal. Bioanal. Chem. 386 (2006) 532–543.
[13] P. Pacher, G. Hajnoczky, Propagation of the apoptotic signal by mitochondrial waves, Embo. J. 20 (2001) 4107–4121.
[14] P. Pacher, A.P. Thomas, G. Hajnoczky, Ca2+ marks: miniature calcium signals in single mitochondria driven by ryanodine receptors, Proc. Natl. Acad. Sci. USA 99 (2002) 2380–2385.
[15] C.J. Lieven, M.J. Hoegger, C.R. Schlieve, L.A. Levin, Retinal ganglion cell axotomy induces an increase in intracellular superoxide anion, Invest. Ophthalmol. Vis. Sci. 47 (2006) 1477–1485.
[16] M.C. Zimmerman, L.W. Oberley, S.W. Flanagan, Mutant SOD1-induced neuronal toxicity is mediated by increased mitochondrial superoxide levels, J. Neurochem. (2007).
[17] A.Y. Abramov, A. Scorziello, M.R. Duchen, Three distinct mechanisms generate oxygen free radicals in neurons and contribute to cell death during anoxia and reoxygenation, J. Neurosci. 27 (2007) 1129–1138.
[18] J. Fauconnier, D.C. Andersson, S.J. Zhang, J.T. Lanner, R. Wibom, A. Katz, J.D. Bruton, H. Westerblad, Effects of Palmitate on Ca^{2+} handling in adult control and ob/ob cardiomyocytes: impact of mitochondrial reactive oxygen species, Diabetes 56 (2007) 1136–1142.
[19] L. Piacenza, F. Irigoin, M.N. Alvarez, G. Peluffo, M.C. Taylor, J.M. Kelly, S.R. Wilkinson, R. Radi, Mitochondrial superoxide radicals mediate programmed cell death in *Trypanosoma cruzi:* cytoprotective action of mitochondrial iron superoxide dismutase overexpression, Biochem. J. 403 (2007) 323–334.
[20] P.R. Castello, D.A. Drechsel, M. Patel, Mitochondria are a major source of paraquat-induced reactive oxygen species production in the brain, J. Biol. Chem. (2007).
[21] J.H. Doroshow, K.J. Davies, Redox cycling of anthracyclines by cardiac mitochondria. II. Formation of superoxide anion, hydrogen peroxide, and hydroxyl radical, J. Biol. Chem. 261 (1986) 3068–3074.
[22] K.J. Davies, J.H. Doroshow, Redox cycling of anthracyclines by cardiac mitochondria. I. Anthracycline radical formation by NADH dehydrogenase, J. Biol. Chem. 261 (1986) 3060–3067.
[23] T. Nishikawa, D. Edelstein, X.L. Du, S. Yamagishi, T. Matsumura, Y. Kaneda, M.A. Yorek, D. Beebe, P.J. Oates, H.P. Hammes, I. Giardino, M. Brownlee, Normalizing mitochondrial superoxide production blocks three pathways of hyperglycaemic damage, Nature 404 (2000) 787–790.